Aerodynamically assisted jet processing of viscous single and multi-phase media‡

S. Arumuganathar[1], S.N. Jayasinghe[1*] and N. Suter[2]
[1]Department of Mechanical Engineering
University College London
Torrington Place
London WC1E 7JE
United Kingdom

[2] Equl Engineering AG
Dufourstrasse
8008 Zurich
Switzerland

Abstract

This paper reports a robust approach for jet processing viscous media in both single and multi-phase. The multi-phase medium (nanosuspension) has nanosized SiO_2 (5nm) particulate material at a loading of ~10 wt.% in suspension. Up until recently aerodynamically assisted jetting had only been applied to the processing of low viscous single phase media. Our investigations demonstrate that it is possible to generate jets from which droplets are initiated by jet fragmentation to the drawing of continuous threads in the micrometer range from the processing of high viscous media (>1000mPa s). The study presents an operational guide of applied pressure – flow rate, demarcations identify regions within the map where droplets and threads are generated together with their respective operational parameters. Hence the effect of applied pressure and flow rate on the jetting process to the generation of droplets to threads together with transmission electron micrographs of the droplet residues forms the discussion in this paper. Our investigation into this jetting approach elucidates and welcomes aerodynamically assisted jetting into the nano- and micro-fabrication arena.

*Corresponding author,
E-mail: s.jayasinghe@ucl.ac.uk
Telephone: +44 (0)2076792960

1. Introduction

Processing sciences play a major role in the rapidly escalating science of today, namely nanoscience[1]. This is predominantly due to the hazardous nature associated with the handling of nanosized particulates together with the freedom to control the fabrication process when such sized particles are in the form of a suspension. Hence the development of processing approaches able to handle nanoparticles in suspension have been earmarked as these techniques have widespread applications and hold the key to the success of nanotechnology.

There are several techniques currently available and those which are rapidly emerging for the handling of such suspensions. These approaches can be segregated categorically by identifying them as jet and non-jet based approaches. Non-jet based approaches for handling nanoparticles in suspensions are used in photolithography techniques where either lasers/stamps or electron beams are used for positioning such particles in suspension to pre-determined locations[2-6]. These techniques have great precision in the nanoscale (<50nm) and are widely used in a whole host of applications ranging from the development of microchips to bio-related applications. Although these approaches operate with high precision and can pattern architectures in both two- and three-dimensions, the techniques require controlled atmospheres and are tremendously costly. Hence such techniques are predominantly used by major chip manufacturers who can both afford the capital cost and the associated running cost of such hi-tech process fabrication technologies.

Contrary to non-jet based techniques, jetting approaches are rapidly evolving and are being recognised as competitive alternatives to non-jet based routes for fabrication. One such technique that has made its debut is ink-jet printing (IJP)[7-9]. This is a technology which is driven by means of a piezoelectric crystal or via a controlled thermal explosion. The process essentially in both cases forces out a droplet through a needle and subsequently this droplet is deposited. Several scientists have focussed on this technology and have developed this droplet production technology together with computer control in the three axes. Hence giving birth to a unique solid freeform fabrication by ink-jet printing approach. This technology has undergone several major developments and today

this technique is capable of handling a wide range of nanomaterials in suspension to the most complex, namely living organisms for the fabrication of tissues and organs for repair[10]. To many ink-jet printing has set the scene and also is used as a benchmark where manifestations and other emerging jet based techniques are developed by. Although this technology is widely used it has an inherent limitation which is based around the needles used and the powder loading in suspension which can be processed employing these fine needles. Generally, ink-jet printing uses needles sized in the 30-60μm which generate droplets which are double the size of the needles. These droplets when deposited increase further in diameter and in most cases are >100μm. Hence in this technique the processing medium viscosity is controlled in relation with the used needles which at best produce droplet residues in the tens of micrometers while avoiding needle blockage.

However, electrosprays, a jetting cousin to IJP is driven by the charging of media within a conducting needle which is later exposed to a high intensity electric field where it jets forming droplets in the nano- and micro-meter size. It is important to note that this jetting route unlike ink-jet printing does not have any relationship between the needle diameter and the generated droplet sizes, which means that needles having large bores could be used for producing fine droplets. Implying the processability of high concentrated particulate suspensions from which droplets sized in the few micrometers are produced[11]. This jetting technology much like ink-jet printing has been coupled with computer control in the three-axes for the development of a solid freeform fabrication route which has been successful in fabricating three-dimensional acritectures[12]. Recently electrosprays have also been unearthed to have the capability of handling living organisms for precision deposition without harming them in anyway[13, 14]. Although the resolutions are comparable with non-jetting technologies this route has the hazardous element of high voltage which is generally, during jetting is in the 1000's of volts. Furthermore, spraying nanosuspensions generate fine droplets containing nanoparticulates which are generally deposited for creating patterns or surface topographyies[15]. However, this does not guarantee that all the generated droplets deposit, as some of these have been reported to re-circulate[16] and can bring a hazardous nature to human health.

In comparison to both jetting technologies, namely, ink-jet printing and electrospraying, aerodynamically assisted jets/jetting (AAJ) does not have limitations suffered by both its cousins in terms of the processability of limited viscosity to the hazardous nature of the high applied voltage, respectively. Hence in this study we show aerodynamically assisted jetting which is driven by means of a pressure difference over an orifice which forms a jet later fragmentating in to droplets an economical and versatile jetting technology which can handle nanosuspensions having high viscosity (never before been demonstrated) for the production of droplets and threads which will significantly influence the drop to thread placement of materials paradigm for the fabrication of structures.

2. Experimental

2.1 Media and materials

The single phase medium used in this study was silicone oil having a viscosity of 1000mPa s (supplied by Polymer Systems Technology Limited, High Wycombe, UK.). The multi-phase medium was prepared in the laboratory by manually mixing measured quantities of nanoparticles (supplied by Nayacol Nanotechnologies Inc., USA) sized 5nm with the silicone oil. The nanosuspension was left to rest after mixing for observing its sedimentation behaviour over two days, which was seen to be negligible. However, the prepared nanosuspension was jetted within an hour of its preparation. The properties of the silicone oil were known as it was provided by the supplier, however the prepared multi-phase media containing the nanosized particles having a loading of ~10wt.% was measured as in our previous work[11], calibration of the equipment was carried out with silicone oil. **Table 1** summarises these properties.

Table 1. Summery of the measured properties of the media investigated in this study

Media	**Viscosity/ mPa s**	**Surface tension/ mNm^{-1}**	**Density/ kgm^{-3}**
Silicone oil	1000	21	970
Nanosuspension	1123	19	1115

2.2 Aerodynamically assisted jetting equipment set-up

The jetting equipment consists of the aerodynamically assisted jetting device (**Figure 1**), which has a chamber of height and internal diameter of 16.2 and 8.2mm respectively made of brass having a threaded needle with an internal diameter of 0.35mm. When fitted the threaded needle is ~ XXmm above the exit orifice. The exit orifice has a diameter of 0.35mm and is counter sunk externally assisting jet formation. In addition to the threaded needle already fitted which holds the flow of the media into the chamber another entrance to the chamber exists which accommodates the flow of compressed air giving rise to the pressure difference over the exit orifice assisting in the formation of a jet. The needle within the chamber holding the flow of media has a syringe connect to it via silicone tubing to a hypodermic needle together with a syringe. The syringe fits firmly on a syringe pump capable of supplying consistent low flow rates of upto 10^{-20} m^3s^{-1} (Model type PHD 4400, HARVARD Apparatus Ltd., Edenbridge, UK). The input of compressed air is regulated via a precision regulator which is digitised and has a resolution of 0.01bar from a compressed air supply of ~6bar.

2.3 Generating an operational guide

An operational guide was generated by investigating a wide parametric space for the applied pressure - flow rate. Our study investigated a range within ~0.01-5bar and 10^{-7}-10^{-10} m^3s^{-1}, respectively. The intension for investigating such a wide parametric space was to identify which operating conditions would allow the production of the finest possible droplets and droplet residues. We initially started by setting the flow rate to the lowest possible flow and applied a pressure which showed the production of droplets but on increasing the applied pressure we observed that jetting seized which was caused by the non-meshing pressure which initiated the flow of compressed air into the syringe ending the jetting and droplet production. Hence the flow of medium was increased and the process was repeated several times till jetting over a wide range was investigated as our motivation for underpinning the operational parameters giving rise to the production of the finest possible droplets was most important.

2.4 Visualisation and characterisation of the jets and droplets

The visualisation of the formed jets to droplets and threads was attained by digital high speed photography with the aid of a MotionXtra HG-100K high-speed camera (capable of capturing 100000fps, supplied by Lake Image Systems Ltd., Hertfordshire**,** UK) having a Sigma 180mm, F3.5 EX DG macro lens together with a halogen lighting source. The captured images were initially stored in the camera and later downloaded to a laptop. These images allowed us to understand the jet fragmentation behaviour of the meniscus for a given flow rate to applied pressure from exit orifice to well below.

2.5 Characterisation of droplets and droplet residues

Employing a Sympatec HELOS/BF-MAGIC laser spectroscopy system, droplet size distributions were analysed at approximately the same distance from the AAJ device exit where droplets were collected for optical microscopy. Droplet and thread collection for optical microscopy was carried out by swiftly moving microslides at a pre-determined distance from the exit orifice. The workings of this laser driven droplet sizer has been previously described[11]. Several different repeated measurements were carried out for each applied pressure to flow rate. The system was calibrated with analysis of generated droplet sizers for a known liquid[17]. In parallel generated droplets and thread residues were characterised as soon as they were collected/deposited on to glass microslides by means of optical microscopy. Subsequently transmission electron microscopy was carried out on collected residues which were deposited on carbon TEM grids having a 300 mesh size. These residues were further examined for there composition by means of both selected area diffraction and energy dispersive x-ray.

3. Results and discussion

3.1 Aerodynamically assisted jetting of the media

Once the AAJ equipment was set-up several permutations and combinations of applied pressure to flow rates were investigated during the generation of the operational guide. Here we identified regions of given effective conditions where the finest possible droplet to droplet residues were

produced and their distributions. The studied parametric operational window had a range of 1-10ml/hour for the flow rate of the media to the needle for a corresponding applied chamber pressure from ~0.01-5bar over the exit orifice.

Initially the flow rate was set to the minimum flow in the regime of 10^{-20} m^3s^{-1} that is the lowest allowed by our present equipment and later the pressure was increased from ~0.01bar. Here we observed that the applied pressure was too large for the selected flow rate and hence resulted in the compressed air flowing into the syringe via the needle holding the media which showed bubbles in the silicone tube flowing into the syringe. We refer to this flow as "back flow" hence the flow rate of the media was increased and was subjected to the same applied pressure, which we repeated till we were able to identify the best flow rates to applied pressures for the generation of the finest possible droplets and residues. Our observations led us to understand that forming of jets from this media took time, we speculate that this is due to the needle wetting together with the associated media properties notably, viscosity. As our previous investigations with media having a viscosity two orders of magnitude smaller formed jets almost instantaneously on applying a pressure[17]. We also noted that for a given applied pressure there is a matching outflow of liquid that is required for forming a jet from which droplets are generated.

3.2 Operational guide

Our study led us to generate an operational guide for an applied pressure ranging from ~0.01-5bar for a corresponding media flow to the needle from 1-10ml/hour. For each flow rate the pressure was increased till back flow was observed which gave rise to the jetting and droplet generation process to seize. **Figure 2a** shows a fenced region in the operational guide for the given needle flow rate where back flow does not occur at those respective applied pressures. Operating within the remit of the fenced region was observed to give rise to the formation of jets which underwent instability initiating the generation of droplets (**Figure 2b**). The operational guide demarks a rather large area for the production of droplets (shaded region). During the generation of this map it was seen that at an applied pressure of ~0.01bar for a flow rate of 5ml/hr the jet formed from the cusp as previously

but did not undergo any instabilities resulting in the formation of a continuous thread. The threading region initiated at 5ml/hour continued even at the flow rate of 10ml/hour for an applied pressure of ≤ 1bar (**Figure 2b**). We believe that this is a direct result of the liquid property viscosity which encourages the media to stretch elastically resulting in the formation of a continuous thread for this demarked region alone. Exiting the threading area introduced the formed jet to initially gently whip as a result of the drag caused by neighbouring air on the jet giving rise to the slowing down of the meniscus which introduces an angular element resulting in the initiation of droplet generation. **Figures 3a** and **b** depict both schematically and via high-speed camera snap shots the droplets and thread generation process respectively.

Crossing the fence in the operational guide from where droplets to threads are formed by collection it was seen the single droplets transforming to droplets with tails to finally continuous threads (**Figures 4a-c**). The generation of droplets and threads within and to their regions were confirmed via collection onto microslides which were analysed by means of optical microscopy on deposition. This was crucial as we wanted to avoid measuring droplets with tails (**Figure 4b**) when droplet sizing was carried out. Throughout this study we allowed the jet to settle for a given operational condition for several minutes before making any measurements.

3.3 Collected droplet and thread residues

On selecting an applied pressure to flow rate demarked in the droplet generation region several minutes were given for the jetting to droplet production process to stabilise. Droplet analysis was carried out by placing the AAJ device in the measurement region of the laser (**Figure 5**) spectrometer where the laser was perpendicular at a distance similar from where droplet collection took place. Several repeated measurements were taken together with optical micrographs of the collected droplets at a similar distance which showed good correlate taking into account, spreading of the droplet deposits on the glass microslides.

The flow rate investigated in this study spanned a flow regime of 10^{-9} m^3s^{-1} hence as the flow rate does not change significantly, it was not surprising that we found for moving along points A, B and C in figure 2b gave rise to a significant plot shift in the droplet size distributions illustrating the generation of smaller droplets with increasing applied pressure (**Figures 6a-c**). Figure 6c also elucidates that the droplet distribution further narrows at these operational conditions. This was also the case for increasing the applied pressure for a given flow rate for the flows 5-10ml/hr. Both droplet residues and threads were measured using optical microscopy. Threading which took place was seen to produce threads which varied from ~200-380μm in diameter. However a systematic study could not be carried out for investigating the thread production of as the region was rather confined to a small operational area.

The deposited multi-phase droplets were found to show optically the aggregation of particles near the central regions of the deposits. Hence, we deposited this media without the applied pressure onto several TEM grids which showed the movement of the particles towards the periphery of the spreading droplet. This is an established phenomenon which forms from the well-known event referred to as the Marangoni effect associate with interactions occurring between adjacent particles or aggregates resulting in the formation of a staggered stair-case like morphology resulting in the formation of a donut shaped architecture with a periphery of aggregated particles (**Figure 7a**)[18-20]. These Marangoni effects are predominant in many nano- and micro-fabrication technologies[21], hampering their abilities when required for fabricating conducting tracks in the case of electrical circuits that require dense structures to applications in the analysis of chemical composition in combitorial chemistry. Contrary to the control deposits the AAJ deposits resulting from the collection of droplets were found to form stable clusters or dense self-assembled structures (**Figure 7b**). From previous work[22] carried out on self-assemblies report that such assemblies are formed as a result of the self-assembling process defined as static assembly giving rise to stable self-assembled structures. In our studies we speculate that there is much mixing (aggressive particulate movement) of the multi-phase media in the formed cone much like those reported in the cones

formed in electrospray studies[23] which gives rise to the densely packed self-assembled stable structures.

These densely formed structures were analysed by means of selected area diffraction which showed clear peaks for silicone and oxygen (**Figure 8a**). Similarly the amorphous nature of this SiO_2 particles where evident on examination of the structures via energy dispersive x-ray analysis (**Figure 8b**).

4. Conclusions

Our investigations have showed that high viscosity liquids both single- and multi-phase can be processed employing aerodynamically assisted jets. The behaviour of these jets for a given flow rate to applied pressure is addressed and elucidated by means of an operational guide showing parameters which would promote the formation of droplets to threads and the finest possible droplets, which could be most useful in the development of this jetting approach as a drop/thread to place type solid freeforming technique. The use of silicone oil not only demonstrates the ability to process high viscosity liquids but its substitution to another polymer having nanoparticulates suspended could be interesting for both production of composite beads to threads which could have significance in targeted drug delivery where the polymer has a known degradation time. The authors hope to couple this jetting device with a purpose built three-axes plotter-like device which would position these droplets and threads for the creation of pre-organised structures via computer control.

‡**Acknowledgements**

SNJ gratefully acknowledges the Engineering and Physical Research Council of the UK for financially supporting this research and a research assistantship for SA via Grant EP/D506964/1. The authors are grateful to Dr. Carl Lance and Dr. David Catone of Nyacol Nanotechnologies. Inc., USA, Mr. Andy Smith of Sympatec, Mr. David Rudeforth of Lake Image Systems Ltd., and both Jackie Goertz and Mr. Derek Williams-Wynn of Polymer Systems Technology Ltd, UK, for all their assistance and support in these investigations.

References

1. G. Ozin, A. Arsenault; Nanochemistry: A Chemical Approach to Nanomaterials, Royal Society of Chemistry, UK., 2005.
2. E. Forsén, P. Carlberg, L. Montelius and A. Boisen, Microelectronic Engineering, 2004, **73–74**, 491.
3. Y.N. Xia and G.M. Whitesides, Annu Rev Mater Sci., 1998, **28**, 153.
4. Y. Lu and S.C. Chen, Advanced Drug Delivery Reviews, 2004, **56**, 1621.
5. J. Taniguchi, K. Koga, Y. Kogo and I. Miyamoto, Microelectronic Engineering, 2006, **83**, 940.
6. A.A. Bettiol, T.C. Sum, F.C. Cheong, C.H. Sow, S.V. Rao, J.A. van Kan, E.J. Teo, K. Ansari and F. Watt, Nuclear Instruments and Methods in Physics Research Section B: Beam Interactions with Materials and Atoms, 2005, **231**, 364.
7. R.A. Street, W.S. Wong, S.E. Ready, M.L. Chabinyc, A.C. Arias, S. Limb, A. Salleo and R. Lujan, Materials Today, 2006, **9**, 32.
8. B-H. Ryu, Y. Choi, H-S. Park, J-H. Byun, K. Kong, J-O. Lee and H. Chang, Colloids and Surfaces A: Physicochemical and Engineering Aspects, 2005, **270-271**, 345.
9. L. Setti, A. Fraleoni-Morgera, B. Ballarin, A. Filippini, D. Frascaro, C. Piana, Biosens Bioelectron., 2005, **10**, 2019.
10. T. Xu, C.A. Gregory, P. Molnar, X. Cui, S. Jalota, S.B. Bhaduri and T. Boland, Biomaterials, 2006, **27**, 3580.
11. S.N. Jayasinghe, Physica E, 2006, **31**, 17.
12. D.Z. Wang, S.N. Jayasinghe and M.J. Edirisinghe, Review of Scientific Instruments, 2005, **76**, 075105.
13. S.N. Jayasinghe and A.N. Qureshi and P.A.M. Eagles, Small, 2006, **2**, 216.
14. S.N. Jayasinghe, P.A.M. Eagles and A.N. Qureshi, Biotechnology Journal, 2006, **1**, 86
15. S.N. Jayasinghe, Physica E, 2006, **33**, 398.

16. R. P. A. Hartman, J. -P. Borra, D. J. Brunner, J. C. M. Marijnissen and B. Scarlett, Journal of Electrostatics, 1999, **47**, 143.

17. S.N. Jayasinghe and N. Suter, Micro and Nano Letters, **in press**.

18. C. Marangoni, Nuovo Cimento Ser 1872, **2**, 239.

19. P.A. Kralchevsky, N.D. Denkov, Current Opin. Coll. Interf. Sci., 2001, **6**, 383.

20. A.D. Nikolov, D.T. Wasan, A. Chengara, K. Koczo, G.a. Policello and I. Kolossvary, Adv. Coll. Interf. Sci., 2002, **96**, 325.

21. J.G.V. Scott, Circ. World 2005, **31**, 34.

22. G.M. Whitesides and B. Grzybowski, Science, 2002, 295, 2418

23. A. Barrero, A. M. Gañán-Calvo, J. Dávila, A. Palacio, and E. Gómez-González, Phys. Rev. E., 1998, **58**, 7309.

FIGURE CAPTIONS

Figure 1. A digital image of the AAJ device employed in this investigation.

Figure 2. a) A guide demarking the region where back flow occurs, b) the operational guide identifying the remit where droplets and threads are generated.

Figure 3. Schematics and high speed snap shots of a) droplets and b) thread generation.

Figure 4. Characteristic micrographs of the collected residues when crossing the fence from a) droplets, b) droplets with tails to finally c) threads.

Figure 5. The aerodynamically assisted jetting device set-up in conjunction with the Sympatec laser droplet sizer.

Figure 6. Characteristic repeated droplets size distributions for a) a flow rate of 1ml/hr and an applied pressure of ~0.3bar – Pt. A, b) a flow rate of 5ml/hr and an applied pressure of 2.5bar – Pt. B, and c) for a flow rate of 10ml/hr and an applied pressure of 5bar – Pt. C.

Figure 7. Typical transmission electron micrographs of a) the controlled droplet deposits and b) the jetted deposits.

Figure 8. Characteristic a) selected area defraction and b) x-ray diffraction of the formed stable self-assemblies by means of this jetting approach.

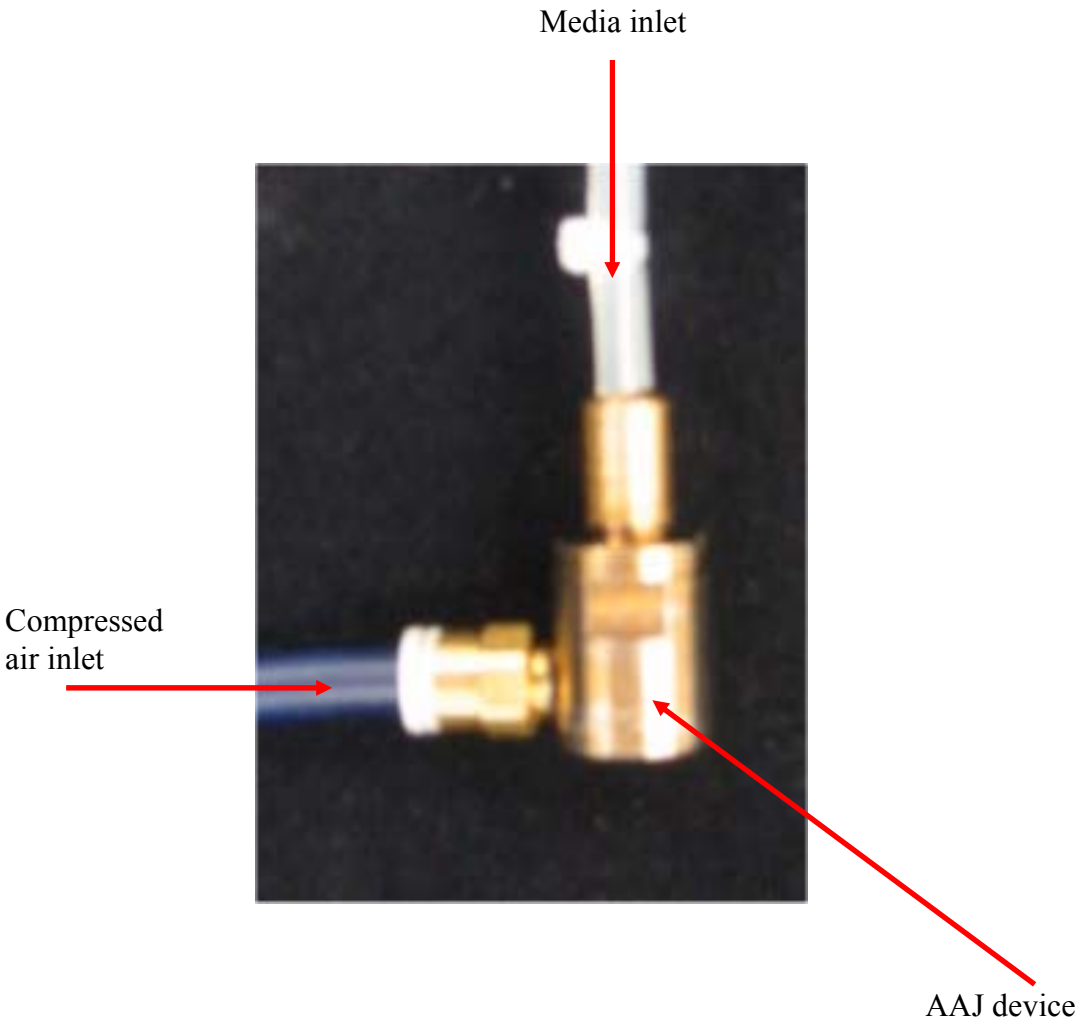

Figure 1

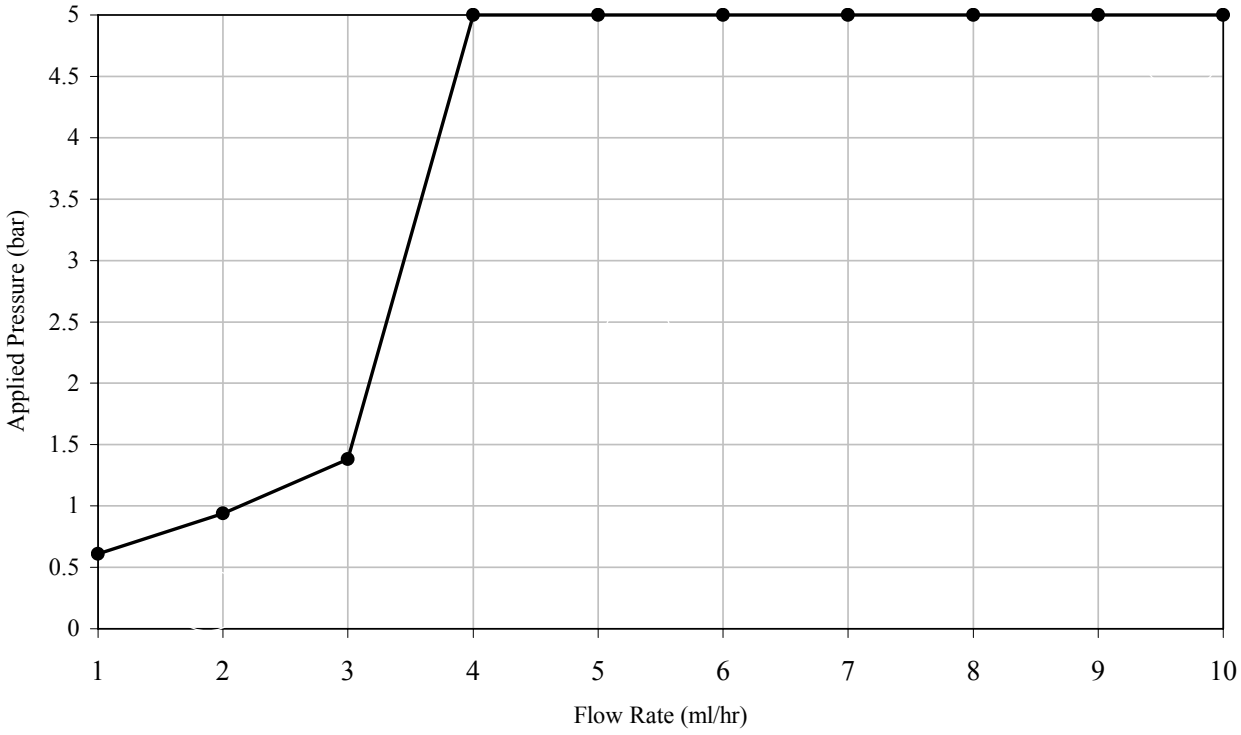

a

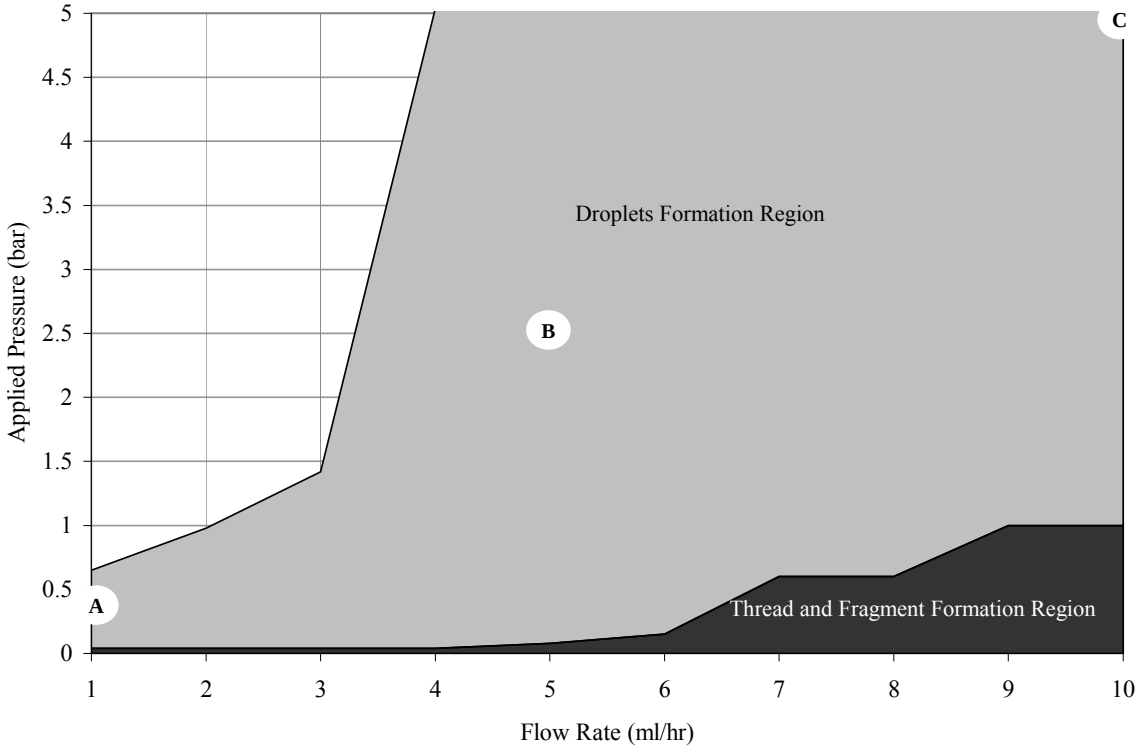

b

Figure 2

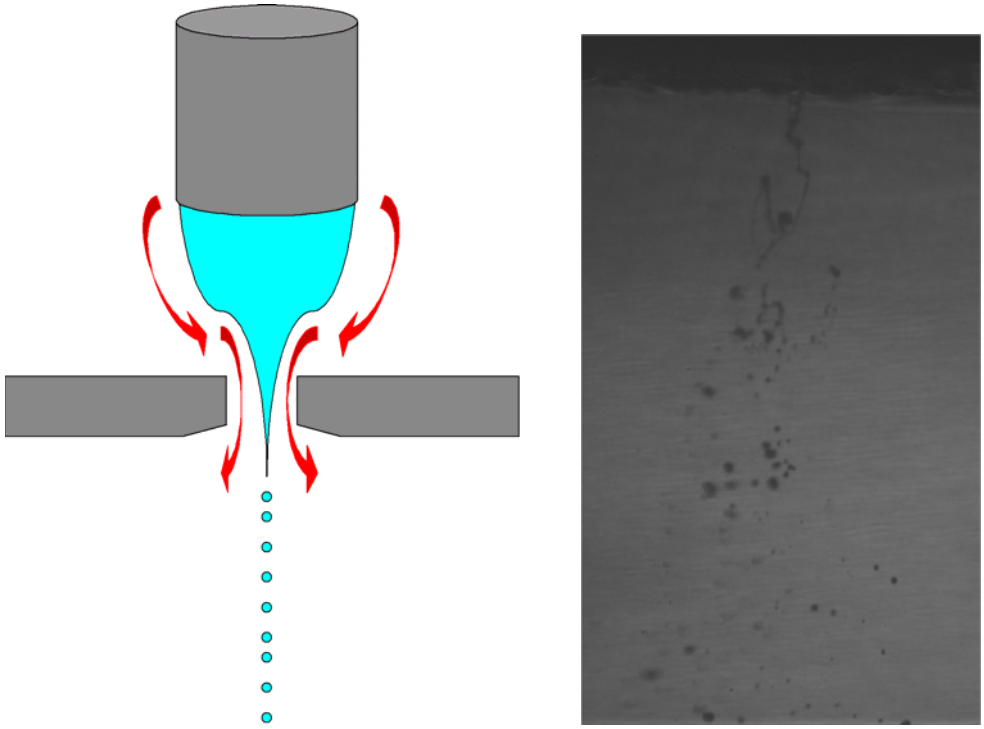

a

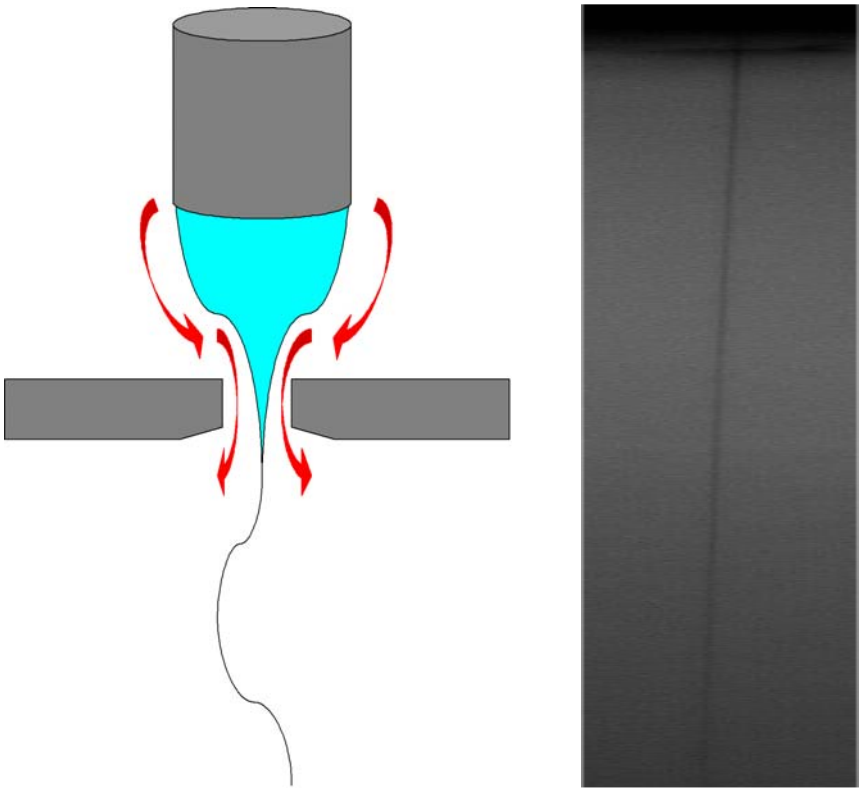

b

Figure 3

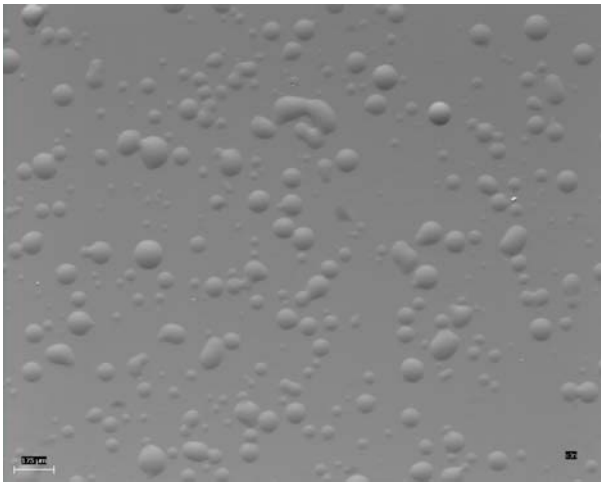

a

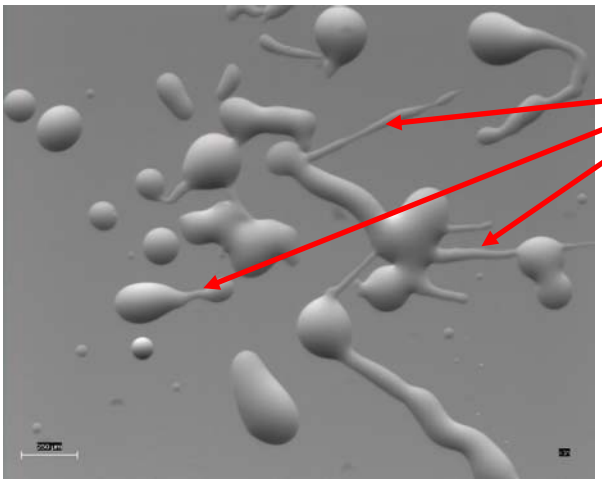

b

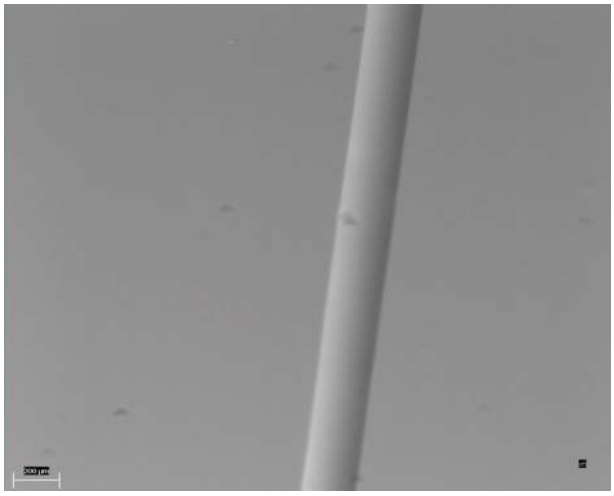

c

Figure 4

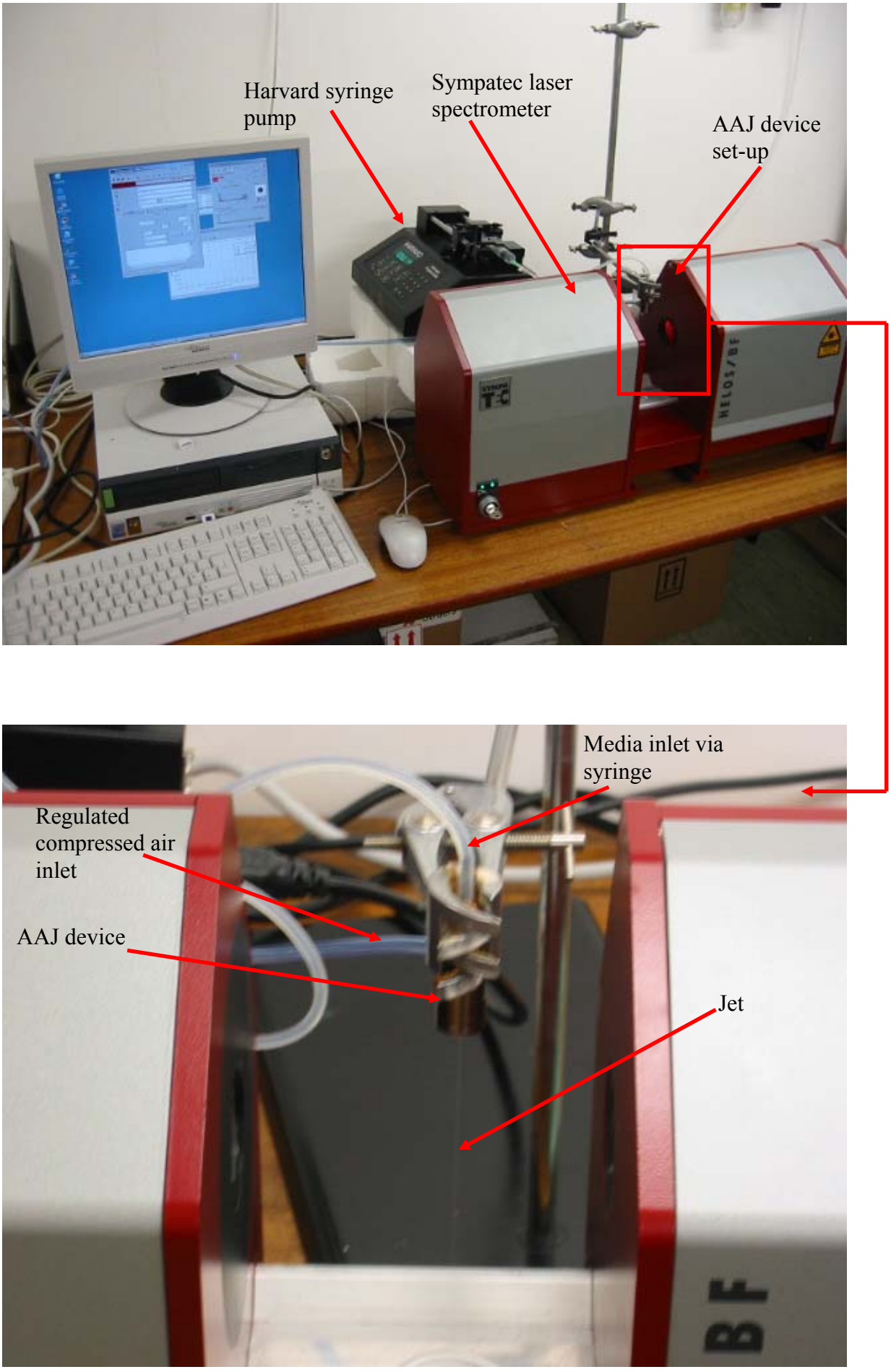
Harvard syringe pump
Sympatec laser spectrometer
AAJ device set-up
Media inlet via syringe
Regulated compressed air inlet
AAJ device
Jet

Figure 5

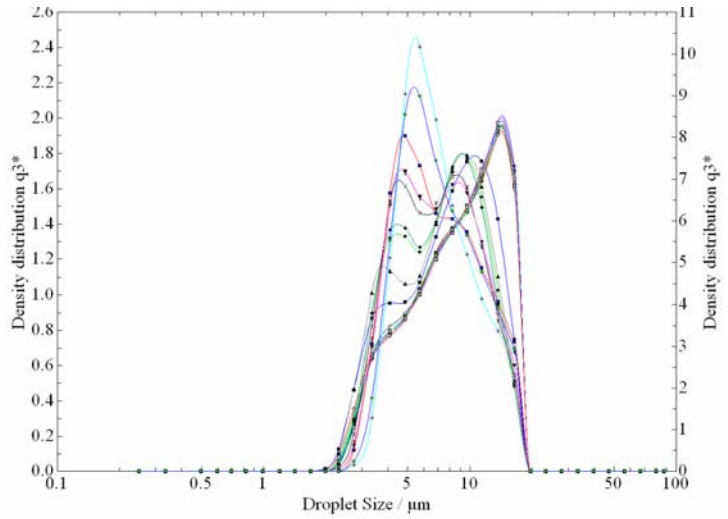
Density distribution q3*
Droplet Size / µm

a

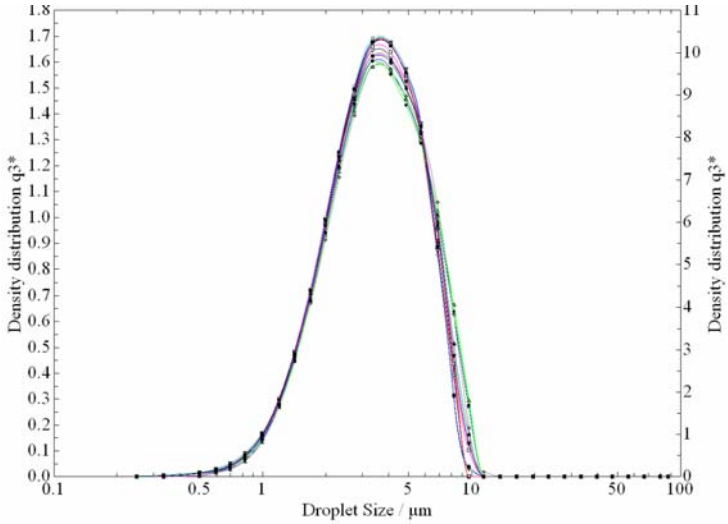
Density distribution q3*
Droplet Size / µm

b

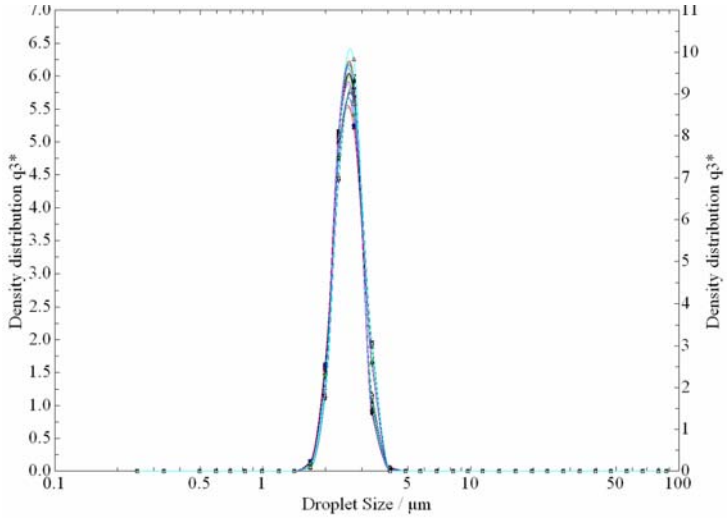
Density distribution q3*
Droplet Size / µm

c

Figure 6

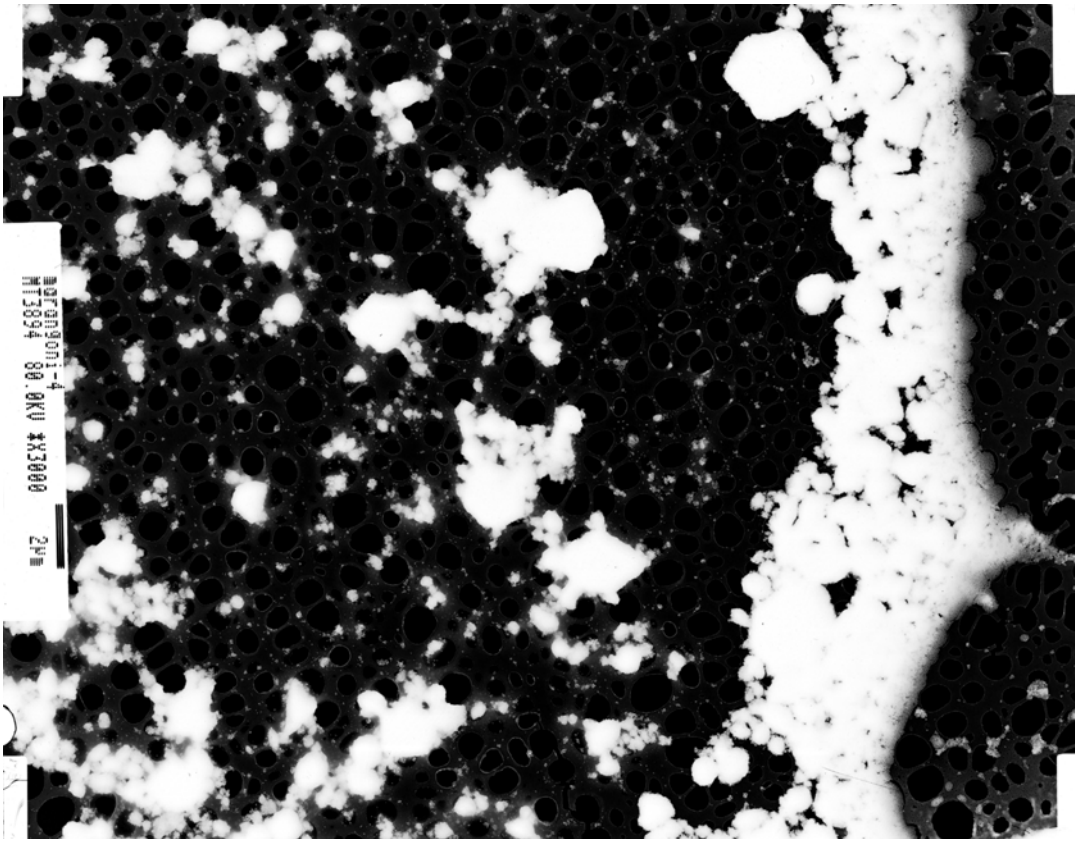

a

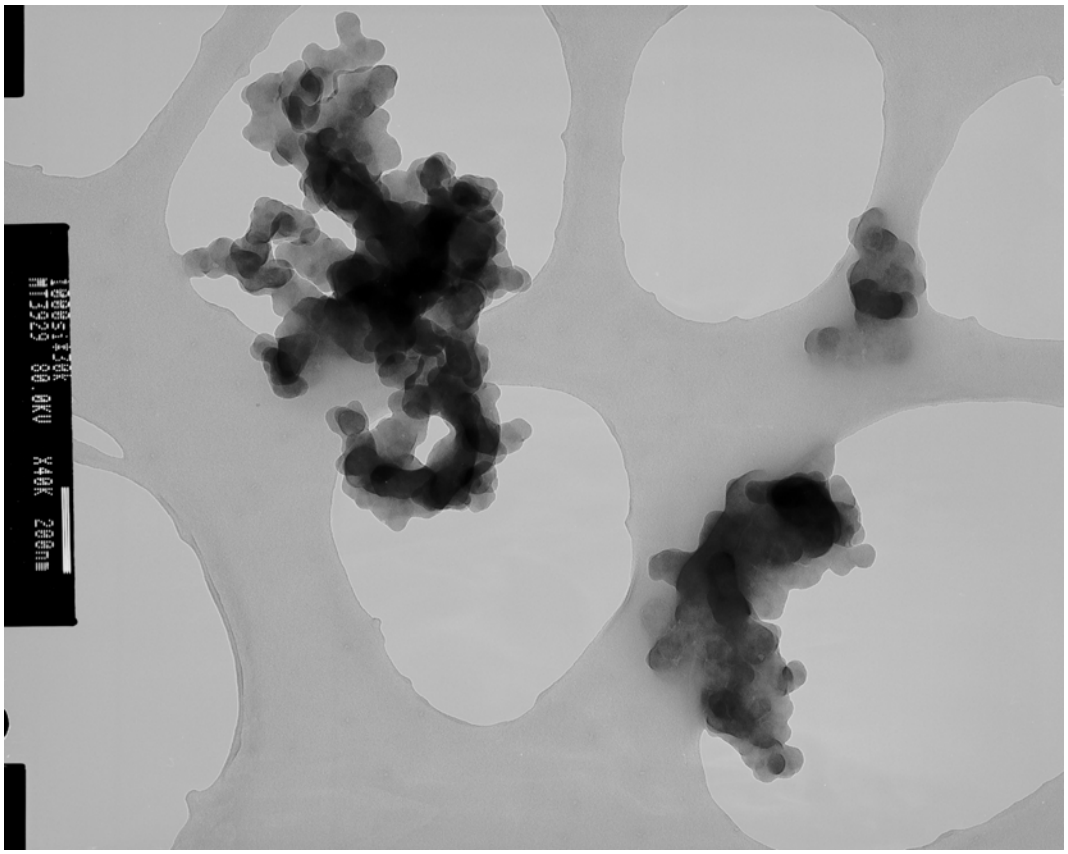

b

Figure 7

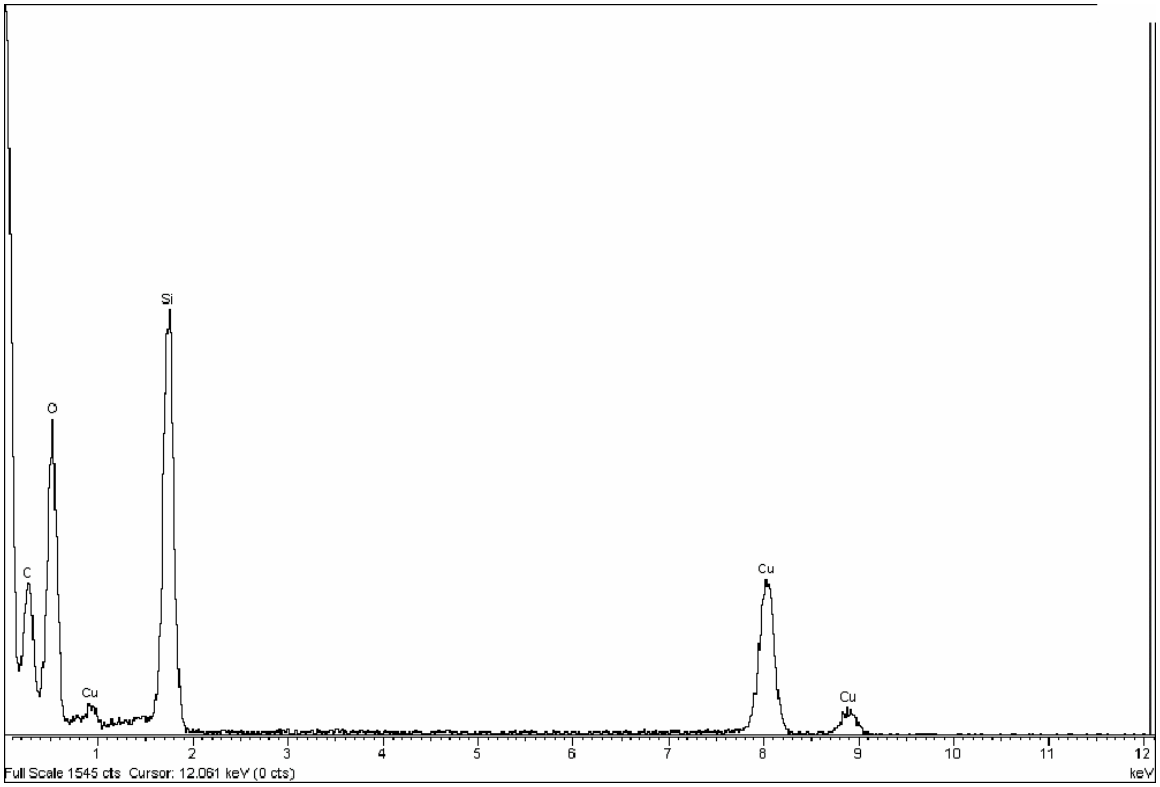
Si
O
C
Cu
Cu
Cu
1
2
3
4
5
6
7
8
9
10
11
12
Full Scale 1545 cts Cursor: 12.061 keV (0 cts)
keV

a

b

Figure 8